ISAR - RADAR IMAGING OF TARGETS WITH COMPLICATED MOTION

T. Sparr

Norwegian Defence Research Establishment (FFI)
Land and Air Systems Division
PO Box 25, N-2027 Kjeller, Norway

ABSTRACT

ISAR imaging is described for general motion of the radar target. ISAR imaging may be seen as a 3D to 2D projection, and the importance of the ISAR image projection plane is stated. For general motion, ISAR images are often smeared when using FFT processing. Time frequency methods are used to analyze such images, and to form sharp images. A given smeared image is shown to be the result of changes both in scale and in the projection plane orientation.

1. INTRODUCTION

Inverse synthetic aperture radar (ISAR) is a technique where a radar image may be formed of a target that rotates relative to the radar [1]. The first systems were used for controlled turntable measurements, and this is still an important technique for high resolution radar cross-section (RCS) measurement. Generally, relative motion between the radar and the target causes an effective rotation of the target as seen from the radar. The effective rotation is a combination of translation-induced aspect change and target internal rotation. The important difference from the turntable is that the target rotation is unknown, and can be complicated [2].

ISAR imaging has mathematical similarities with computed tomography as used in medical and other applications [3]. In such a description, projections play an important role. Radar range profiles are 3D to 1D projections, and the usual challenge is to construct a 2D image from the 1D projections. There is a potential for making 3D images [2], but this is feasible only for motions resulting in projections that cover 3D spatial frequency domain. If the motion is fairly simple, only 2D images are useful.

The traditional way to describe ISAR imaging is using the range-Doppler formulation [4]. Here, a scatterer on the target is located in range using radar range resolution, and in cross-range using Doppler resolution. Considering general cases, projections still play an important role, and the concept of an ISAR projection plane is useful. We review some results from the last few years considering target motion, projection and image smearing.

The study was partly funded by grant N01-25 from US Office of Naval Research through the "Naval International Cooperative opportunities in Science and Technology Program (NICOP)." The author thanks Dr William B. Miceli at ONR Global, London, for the support.

2. RANGE-DOPPLER ISAR

2.1. Imaging System Model

ISAR imaging requires that the target rotates relative to the radar, so that projections of the target may be formed from different angles. A radar high resolution rangeprofile is the projection of the 3D target scattering distribution down onto a 1D line in the range direction. Accordingly, the distances to the scattereres are measured using the radar range resolution, but all scattereres that are within a shell with the thickness of the range reolution, sum coherently and appear in the same cell in the range profile. When the target rotates, consecutive range profiles are seen from slightly different angles, and the projections become different. Reconstructing the 2D or 3D target structure from the projections is the heart of ISAR imaging.

When the target rotation is simple as for a turntable system [1], the image formation is quite easy. For sufficiently small angles of rotation, FFT-based range-Doppler processing is enough. Real targets such as boats, ground vehicles and aircraft are different [5, 6, 7]. Due to the target motion, the effective rotation is not like a turntable at all. Instead, the rotation is described by the angular velocity vector, a vector with three in general time dependent components [5]

$$\boldsymbol{\omega}(t) = [\omega_1(t), \omega_2(t), \omega_3(t)]^T. \quad (1)$$

It is convenient to define a coordinate system with the x-axis along the radar boresight as shown in Fig. 1. The origin is chosen to be coincident with the center of rotation of the target. When this is the case, and the rotation is sufficiently small, the Doppler shift corresponding to a scatterer in position $\mathbf{r}_0 = [x_0, y_0, z_0]^T$ with respect to the target body

0-7803-8554-3/04/$20.00 ©2004 IEEE.

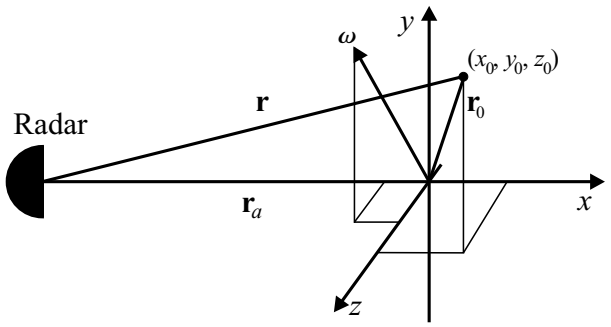

Fig. 1. The geometry for ISAR imaging when target 3D structure and general rotation is taken into account.

coordinates may be found as

$$\begin{aligned} f_d &\approx (2/\lambda)\,(\omega_3 y_0 - \omega_2 z_0) \\ &= (2/\lambda)\,|\boldsymbol{\omega}_\perp \times \mathbf{r}_{0\perp}| \\ &= (2/\lambda)\;\omega_\perp r_{0\perp} \sin\alpha, \end{aligned} \tag{2}$$

with $\boldsymbol{\omega}_\perp = [0, \omega_2, \omega_3]^T$ and $\mathbf{r}_{0\perp} = [0, y_0, z_0]^T$, the components of the angular velocity and the scatterer position perpendicular to the radar range direction. We see that the ω_1-component of the angular velocity does not cause any Doppler shift. The reason is that a pure rotation around the radar boresight does not change scatterer distance from the radar. The usual 2D turntable formulation corresponds to $\omega_3(t) = \Omega$, a constant, and $\omega_2 = 0$, giving $f_d = 2\Omega y_0/\lambda$.

2.2. ISAR Imaging Projection Plane

It is clear from the previous section that a scatterer may be positioned in range using the radar range resolution, and in cross-range using the Doppler frequency. Accordingly, it is possible to obtain an image of the radar scattering, a two-dimensional representation of the electromagnetic scattering properties of the target. The normal vector giving the ISAR projection plane is found simply as

$$\hat{\mathbf{n}} = \frac{\boldsymbol{\omega}_\perp}{|\boldsymbol{\omega}_\perp|}. \tag{3}$$

The scaling factor between distance in the projection plane and measured Doppler frequency is equally simple

$$d = \frac{\lambda}{2\,|\boldsymbol{\omega}_\perp|} f_d. \tag{4}$$

Accordingly, it is easy to from an image when the angular veloity vector is simple. The traditional FFT-based processing requires constant angular velocity. But the angular velocity is often a complicated function. For ground targets and aircraft, manoeuvres cause complicated rotation, while ships are affected by wave motion. An example [5] is given in figure 2. Two ISAR images formed using conventional FFT-based processing are given. They are formed from consecutive blocks of radar data, but the difference is striking. One image (upper) is reasonably focused, and it is easy to recognize the outline of an aircraft. The other (lower) is by comparison smeared. The smearing is caused by two effects. The first is that the angular velocity vector magnitude changes during the time of integration. This changes the scaling. The second is that the angular velocity vector changes direction. This changes the ISAR projection plane.

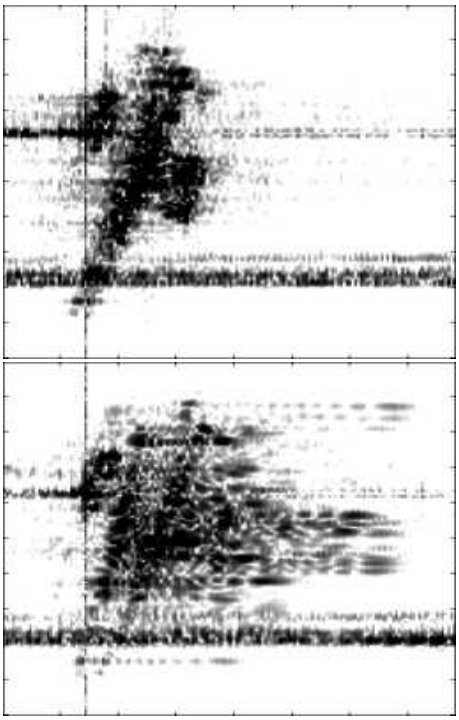

Fig. 2. Two ISAR images formed using conventional ISAR processing. Range is along the y-axis and cross-range (Doppler) is along the x-axis.

As seen from equation (2), changes in both the angular velocity vector magnitude $\omega_\perp$ and in the angle between the angular velocity vector and the position vctor of the scatterer α affect the Doppler shift. Particularly the angle α can be very sensitive to target manoeuvres. Spectacular examples of this effect has been shown for ISAR imaging of ships [7].

3. TIME-FREQUENCY ISAR

Time-frequency methods offer an advantage over conventional FFT-based methods when analyzing complicated cases [8, 9]. However, it is well known that choosing a method is

not an easy task [10]. Considering the demands posed by an ISAR processor of both the highest possible resolution and, at the same time sufficient dynamic range to take into account the high variability of reflector strength on man-made targets, it seems clear that the class of quadratic methods is best. The class of quadratic methods is known as the Cohen's class. This class holds the promise of full resolution, even for time-varying signals. The Cohen's class are all described by [11]

$$C(t, f_d) = \int_{-\infty}^{\infty} \int_{-\infty}^{\infty} W(u, v)\Psi(u-t, v-f_d)\, \mathrm{d}u\, \mathrm{d}v. \quad (5)$$

Here, $W(t, f_d)$ is the baseline Wigner-Ville distribution

$$\begin{array}{l} W(t, f_d) \\ = \int_{-\infty}^{\infty} s(t+\tau/2)s^*(t-\tau/2) \exp(-j2\pi f_d \tau)\, \mathrm{d}\tau. \end{array} \quad (6)$$

Hence, all the instances of Cohen's class may be seen as the Wigner-Ville distribution convolved with various kernels Ψ. Relevant choices are smoothing kernels that reduce the high level of interference between various components of the basic signal $s(t)$. For efficiency, the smoothing can be carried out on the ambiguity function which is the 2D Fourier transform of the Wigner-Ville distribution. In this domain, the convolution becomes a multiplication. Depending on the choice of kernel, we trade between resolution and interference level. The baseline Wigner-Ville is known to perfectly localize the time-frequency content of a single linear chirp, but with almost any other kind of signal, the interference makes it next to useless. At the other end of the scale is the short-time Fourier transform (STFT) that has almost no interference problems. The resolution is, however, coarse compared with other methods. Still, the STFT is very useful for the applications where the resolution is adequate.

A first-try quadratic method that we often find useful, is the smoothed pseudo Wigner-Ville distribution (SPWVD). The SPWVD is an example of a Cohen's class distribution, where the kernel function is separable to provide independent smoothing in time and frequency. The expression for the SPWVD is [12]

$$\begin{array}{l} SPW(t, f_d) \\ = \int_{-\infty}^{\infty} h(\tau) \int_{-\infty}^{\infty} g(s-t)x(s+\tau/2) \\ \times x^*(s-\tau/2)\, \mathrm{d}s\, \exp(-j2\pi f_d \tau)\, \mathrm{d}\tau. \end{array} \quad (7)$$

We are free to choose the length and type of the smoothing windows $g(t)$ and $h(t)$. A typical choice is the Hamming window, which we use in the following.

Using the SPWVD on each range line of the blurred image, we obtain a stack of images corresponding to the one we get from FFT based processing. Three examples are given in figure 3. Between the first and the last image, we see mainly a scaling change, and we can assume only a change of angular velocity magnitude. By comparison, the middle image shows distortion (effectively different scale changes for different scatterers), and we conclude that the projection plane also changes. The smearing may thus be explained by change in scaling and projection plane during the time of integration for the FFT-based processing.

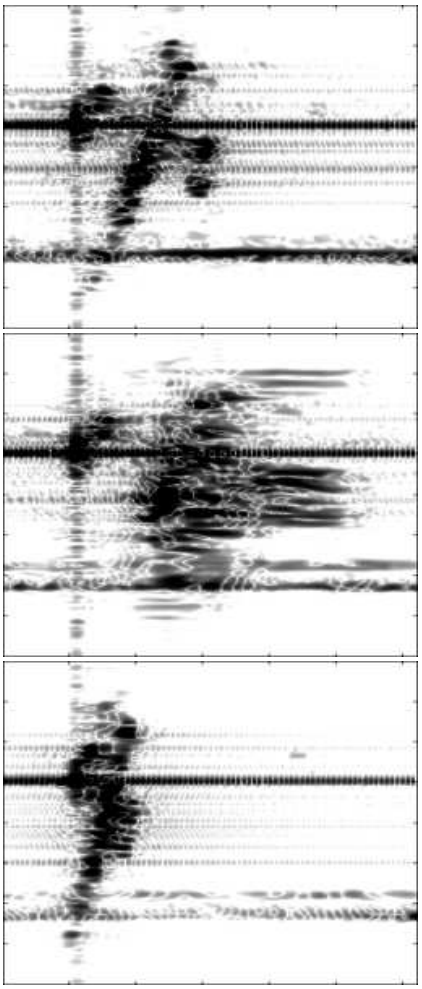

Fig. 3. Time-frequency images at three different times during the coherent integration time of the blurred image.

4. CONCLUSIONS

ISAR imaging is a method where target rotation makes it possible to generate a radar image of the target. The effective rotation is caused by translation as well as target internal rotation. ISAR imaging may be seen as a 3D to 2D projection, and the projection plane normal vector is given by the angular rotation vector of the target. When target motion is complicated during the time of integration, conventional images are smeared. A time-frequency method is then an attractive alternative, as such methods have the

potential for revealing the changing frequencies caused by the motion. An example was given, showing that smearing could be explained by changes in the projection during the time of intergration.

5. REFERENCES

[1] Jack L. Walker, "Range-doppler imaging of rotating objects," *IEEE Trans. on Aerospace and Electronic Systems*, vol. AES-16, no. 1, pp. 23–52, Jan. 1980.

[2] Roger J. Sullivan, *Microwave Radar: Imaging and Advanced Concepts*, Artech House, Inc., Norwood, Massachusetts, 2000.

[3] Charles V. Jakowatz, Jr., Daniel E. Wahl, Paul H. Eichel, Dennis C. Ghiglia, and Paul A. Thompson, *Spotlight-Mode Synthetic Aperture Radar: A Signal Processing Approach*, Kluwer Academic Publishers, Dordrecht, 1996.

[4] Dale A. Ausherman, Adam Kozma, Jack L. Walker, Harrison M. Jones, and Enrico C. Poggio, "Developements in radar imaging," *IEEE Trans. on Aerospace and Electronic Systems*, vol. AES-20, no. 4, pp. 363–399, July 1984.

[5] Trygve Sparr, "Time-frequency techniques applied to ISAR imaging of aircraft," *SPIE Proceedings on Wavelet Applications*, vol. 4391, pp. 35–43, 2001.

[6] John C. Kirk, Jr., "Options for time-frequency processing in ISAR ATR," *SPIE Proceedings on Wavelet Applications*, vol. 4391, pp. 358–369, 2001.

[7] Victor C. Chen and Ronald Lipps, "ISAR imaging of small craft with roll, pitch and yaw analysis," in *The Record of the IEEE International Radar Conference 2000*, 2000.

[8] Victor C. Chen and Hao Ling, "Joint time-frequency analysis for radar signal and image processing," *IEEE Signal Processing Magazine*, pp. 81–93, Mar. 1999.

[9] Trygve Sparr, Svein-Erik Hamran, and Erik Korsbakken, "Estimation and correction of complex target motion effects in inverse synthetic aperture imaging of aircraft," in *The Record of the IEEE International Radar Conference*, 2000.

[10] Gonzalo R. Arce and Syed Rashid Hasan, "Eliminiation of interference terms of the discrete wigner distribution using nonlinear filtering," *IEEE Trans. on Signal Processing*, vol. 48, no. 8, pp. 2321–2331, Aug. 2000.

[11] Leon Cohen, *Time-Frequency Analysis*, Prentice Hall PTR, Upper Saddle River, New Jersey, 1995.

[12] François Auger, Patrick Flandrin, Paulo Gonçalvès, and Olivier Lemoine, *Time-Frequency Toolbox for Use with MATLAB*, 1996.